RASĀYAN *J. Chem.*
Vol. 19 | Special Issue | 197-207 | 2026
ISSN: 0974-1496 | e-ISSN: 0976-0083 | CODEN: RJCABP
http://www.rasayanjournal.com
http://www.rasayanjournal.co.in

COMPARATIVE GREEN BIOSYNTHESIS AND PHYSICOCHEMICAL CHARACTERIZATION OF COPPER AND MAGNESIUM NANOPARTICLES USING *Aspergillus oryzae* CELL CULTURE AND *Zingiber officinale* EXTRACT

N. A. Dibua[1,2], E. I. Chukwura[2], I. O. Emmy-Egbe[3], B. O. Uba[1], F. O. Nwajiobi[2], I. S. Ezenwata[3], O. H. Obiefuna[1], E. C. S. Okoye[1], C. J. Chikwendu[4], L. C. Eleanya[1], S. C. Afulukwe[5], and C. Egbuna[4,6,✉]

[1]Department of Microbiology, Faculty of Natural Sciences, Chukwuemeka Odumegwu Ojukwu University, Uli Campus, Anambra State, Nigeria
[2]Department of Applied Microbiology & Brewing, Faculty of Biosciences, Nnamdi Azikiwe University, Awka, Anambra State, Nigeria
[3]Department of Biological Sciences, Faculty of Natural Sciences, Chukwuemeka Odumegwu Ojukwu University, Uli Campus, Anambra State, Nigeria
[4]Department of Biochemistry, Faculty of Natural Sciences, Chukwuemeka Odumegwu Ojukwu University, Uli Campus, Anambra State, Nigeria
[5]Department of Medical Laboratory Science, Chukwuemeka Odumegwu Ojukwu University, Anambra State, Nigeria
[6]Africa Centre of Excellence in Public Health and Toxicological Research (ACE-PUTOR), University of Port-Harcourt, Port Harcourt, Rivers State, Nigeria
✉Corresponding authors: egbunachukwuebuka@gmail.com

ABSTRACT

The growing demand for environmentally sustainable nanomaterials has increased interest in biological nanoparticle synthesis. This study compared the green synthesis and physicochemical properties of copper and magnesium nanoparticles produced using *Aspergillus oryzae* cell culture and *Zingiber officinale* (ginger) extract as biological reducing and stabilising agents. Nanoparticle formation was initially indicated by colour changes and subsequently confirmed through scanning electron microscopy (SEM), X-ray diffraction (XRD), Fourier-transform infrared (FTIR) spectroscopy, and ultraviolet–visible (UV–Vis) spectroscopy. UV–Vis analysis showed maximum absorption at 550 and 400 nm for *A. oryzae*-mediated copper and magnesium nanoparticles, respectively, and at 500 and 400 nm for ginger-mediated copper and magnesium nanoparticles. FTIR analysis revealed hydroxyl, carbonyl, amine, methoxy, aldehyde, and aromatic groups, suggesting their involvement in metal-ion reduction and nanoparticle stabilisation. XRD confirmed crystallinity, with average crystallite sizes of 7.24 and 7.43 nm for fungal-derived copper and magnesium nanoparticles, respectively, compared with 59.4 and 23.0 nm for the corresponding ginger-derived nanoparticles. SEM revealed predominantly irregular particles measuring 50–83.5 nm, with fungal-derived magnesium nanoparticles showing the smallest average size. Both biological systems successfully produced stable nanoparticles, although *A. oryzae* provided greater control over crystallite and particle size. Green fungal and plant-mediated synthesis therefore offers a sustainable approach for potential biomedical, agricultural, and environmental applications.

Keywords: Green Synthesis, Copper Nanoparticles, Magnesium Nanoparticles; *Aspergillus Oryzae*, *Zingiber Officinale*, Nanoparticle Characterisation, FTIR.

RASĀYAN *J. Chem.*, Thematic Issue, 2026

INTRODUCTION

As a field, nanotechnology has reshaped materials science in the twenty-first century through its ability to engineer matter at the nanoscale, producing physicochemical, optical, catalytic, electrical, and biological behaviours that bulk materials do not display. Particles within the 1-100 nm range gain a markedly higher surface-area-to-volume ratio, greater surface reactivity, quantum confinement phenomena, and functional

This work is licensed under a CC BY 4.0 license.

versatility, which together underpin their growing relevance in environmental remediation, agriculture, medicine, food technology, electronics, and energy.[1] Building on these properties, metallic and metal oxide nanoparticles have advanced rapidly as candidates for targeted drug delivery, biosensing, antimicrobial formulation, catalysis, wastewater treatment, crop improvement, and cancer therapy.[2,3] Among the various classes of engineered nanomaterials, metallic nanoparticles stand out for their biocompatibility, broad-spectrum antimicrobial action, antioxidative capacity, and strong catalytic performance. Copper nanoparticles (CuNPs) are especially attractive because they combine a relatively low production cost with high electrical conductivity, catalytic efficiency, antioxidant behaviour, and marked activity against a wide range of pathogenic microorganisms. Magnesium and magnesium oxide nanoparticles (MgNPs/MgO NPs), for their part, offer strong biodegradability, low toxicity, high thermal stability, and notable anti-inflammatory, antioxidant, and anticancer effects, all of which make them attractive for environmental and biomedical use.[4,5] Conventional physicochemical methods for nanoparticle synthesis, often require hazardous reducing agents, expensive instrumentation, elevated temperatures, and high energy consumption. These approaches frequently generate environmentally hazardous by-products and may leave toxic residues on nanoparticle surfaces, thereby limiting their biomedical and environmental.[1,5] Furthermore, concerns regarding nanoparticle-associated toxicity have intensified the search for environmentally benign synthesis routes. Although nanoparticles offer enormous therapeutic and technological benefits, their interactions with biological systems may cause inflammation, oxidative stress, DNA damage, organ toxicity, and cellular dysfunction depending on their composition, size, concentration, and surface chemistry.[6] Green synthesis has therefore become an appealing alternative to traditional nanoparticle production by utilizing naturally occurring biomolecules as reducing, stabilizing, and capping agents. Green synthesis is more affordable, scalable, energy-efficient, and environmentally friendly than conventional approaches. It can also produce extremely stable nanoparticles with better biocompatibility and less of an influence on the environment.[5,7] Diverse metabolites, including proteins, polysaccharides, amino acids, enzymes, flavonoids, phenolics, terpenoids, alkaloids, and organic acids, are found in biological systems such as microorganisms and plants. Such metabolites help reduce metal ions and stabilise nanoparticles without the use of dangerous chemicals.[7,8] These naturally occurring metabolites not only simplify nanoparticle synthesis but also improve particle stability, dispersibility, and biological functionality. Despite the increasing number of reports on fungal- and plant-mediated nanoparticle synthesis, most published studies have focused on a single biological source or a single metallic nanoparticle, particularly silver nanoparticles. Comparative investigations evaluating different biological reducing systems for synthesizing multiple metallic nanoparticles under similar experimental conditions remain relatively limited. Moreover, relatively few studies have systematically compared the physicochemical characteristics of copper and magnesium nanoparticles synthesized using fungal extracellular metabolites and plant phytochemicals. Since the biological reducing agent strongly influences nucleation, crystal growth, particle morphology, crystallinity, surface functionalization, and optical properties, comparative studies are essential for identifying the most efficient biological systems for producing nanoparticles with desirable characteristics for specific biomedical and environmental applications.[1,5] Building on this gap, the present work drew on extracts of *Zingiber officinale* alongside extracellular metabolites from *Aspergillus oryzae* cell culture to compare how each route drives the green biosynthesis of copper and magnesium nanoparticles. By setting fungal- and plant-mediated synthesis side by side, the study contributes to the case for sustainable, biologically compatible nanomaterials suited to future biomedical, agricultural, and environmental use, while also clarifying how the choice of biological reducing agent shapes nanoparticle formation and physicochemical behaviour.

EXPERIMENTAL

Materials and Methods

Isolation and Molecular Identification of the Fungal Isolate

The fungal strain employed for nanoparticle synthesis was isolated from soil and tentatively identified on the basis of its colony morphology and microscopic characteristics. Purified genomic DNA from the isolate served as a template for polymerase chain reaction using the universal primers ITS1 (5′-TCCGTAGGTGAACCTGCGG-3′) and ITS4 (5′-TCCTCCGCTTATTGATATGC-3′); the amplicons

generated were subsequently sent for sequencing. To establish the isolate's taxonomic identity, the resulting sequences were compared against entries deposited in the NCBI database using the BLAST algorithm, and a phylogenetic tree was built to support the classification.

Preparation of *Zingiber officinale* Extract

Fresh rhizomes of *Z. officinale* were washed several times under running distilled water to eliminate residual soil, sliced into smaller pieces, and left to air-dry in the shade prior to processing. Once dried, the material was milled to a fine powder, mixed with distilled water, and subjected to controlled heating to facilitate the release of its bioactive constituents. The resulting mixture was passed through Whatman No. 1 filter paper, and the clarified filtrate was refrigerated at 4°C until required for use as the reducing and stabilizing agent in the subsequent nanoparticle synthesis.

Green Biosynthesis of Copper and Magnesium Nanoparticles

The biosynthesis of copper and magnesium nanoparticles was achieved by employing *A. oryzae* cell-culture filtrate together with *Z. officinale* extract as reducing agents. Solutions of Copper(II) nitrate trihydrate and magnesium chloride hexahydrate were separately treated with the fungal filtrate and the ginger extract, with continuous stirring maintained throughout. The reaction mixtures were allowed to incubate until a noticeable shift in colour indicated that the metal ions had been reduced and nanoparticles had begun to form. Following synthesis, the nanoparticles were recovered by centrifugation, washed several times with distilled water, and dried in readiness for further physicochemical characterisation.

Characterisation of Biosynthesised Nanoparticles

Visual Observation

An initial, qualitative indication of copper and magnesium nanoparticle formation was provided by distinct colour changes observed in the reaction mixtures, corresponding to the reduction of metal ions into their nanoparticle state.

UV–Visible Spectroscopy

The optical absorption characteristics of the biosynthesised nanoparticles were assessed by scanning them with a UV–Visible spectrophotometer over an appropriate wavelength window. Peak absorption wavelengths recorded during this analysis served to verify nanoparticle formation and to characterize their optical behaviour.

Fourier Transform Infrared (FTIR) Spectroscopy

To identify the biomolecules responsible for reducing, capping, and stabilising the nanoparticles, FTIR analysis was performed. Spectral data were acquired across the range of 500–4000 cm^{-1}, and individual absorption peaks were assigned to their respective functional groups.

X-ray Diffraction (XRD) Analysis

The crystalline nature of the synthesised nanoparticles was investigated using X-ray diffraction, and the mean crystallite size was determined from the diffraction data obtained across the appropriate 2θ range.

Scanning Electron Microscopy (SEM)

Scanning electron microscopy (SEM) was employed to evaluate the surface morphology and particle dimensions of the biosynthesised nanoparticles. The micrographs obtained were analysed to determine particle shape, surface texture, degree of aggregation, and average particle size.

Statistical Analysis

Each experiment was conducted in three independent replicates, and data are presented as mean ± standard deviation (SD). Group differences were evaluated using analysis of variance (ANOVA), with a P-value of less than 0.05 taken to indicate statistical significance.

RESULTS AND DISCUSSION

Molecular Identification of the Fungal Isolate

Morphological and cultural assessment revealed that the soil-derived isolate formed brown-to-dark conidia atop a yellowish-green colony of irregular shape, characterized by a flat elevation and a smooth margin

(Table-1) — features consistent with the genus *Aspergillus*. Successful amplification of the target locus was achieved by targeting the internal transcribed spacer (ITS) region of the fungal rDNA using the universal primers ITS1 (5′-TCCGTAGGTGAACCTGCGG-3′) and ITS4 (5′-TCCTCCGCTTATTGATATGC-3′). This reaction yielded a single amplicon of approximately 500 bp, as confirmed by 1% agarose gel electrophoresis (Plate 1). BLAST analysis of the sequenced amplicon against the NCBI nucleotide database returned *A. oryzae* as the top hit, with 99.28% E-value of 0.0 and sequence identity (Table-2; GenBank accession MH345902.1). Phylogenetic reconstruction placed the isolate within a well-supported clade containing reference *A. oryzae* sequences (bootstrap value 71), distinct from the *Marasmiellus sp*. outgroup (Fig.-1), corroborating the molecular identification.

Table-1: Morphological Characteristics of the Isolated Fungus from the Soil

Characteristics	Colonial description
Colour	Yellowish green
Shape of colony	Irregular
Elevation	Flat
Margin	Smooth

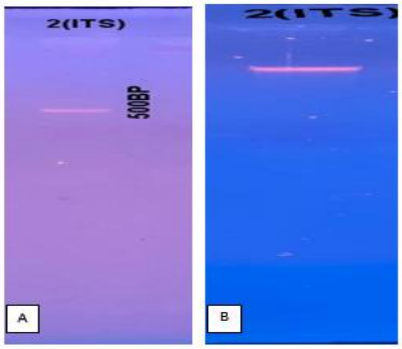


Plate-1: (a) PCR Amplification(b)Gel Electrophoresis of the ITS rRNA Gene of the *Aspergillius oryzae G*enome

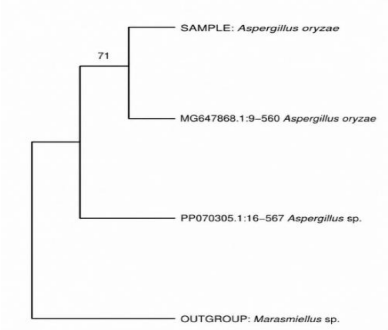


Fig.-1: Phylogenic Tree Showing the Relationship of *A. oryzae* to Similar Fungi of the Same Ancestry

Table-2: BLAST Profile of ITS rRNA Sequences of the Isolated Fungus with Reference Sequences from NCBI

Sample Name	Sequence Source Organism (Top Hit)	Percentage Identification	E-Value	Accession No
FS	*A. oryzae*	99.28%	0.0	MH345902.1

Green Biosynthesis of Copper and Magnesium Nanoparticles

Visual Observation of Nanoparticle Formation

The biosynthesis of the copper and magnesium nanoparticles was first confirmed visually through a distinct colour change in the reaction mixtures following titration of the metal salt solutions with the biological extracts. For the *A. oryzae*-mediated synthesis, the copper (II) nitrate trihydrate solution changed from blue to green, while the magnesium chloride hexahydrate solution changed from colourless to golden. A similar pattern was observed for the ginger (*Z. officinale*)-mediated synthesis, with the copper nitrate solution changing from blue to green and the magnesium chloride solution changing from colourless to golden. These colour changes, summarized in Table-3, indicated the bioreduction of the metal ions and the biosynthesis of copper and magnesium nanoparticles in both the fungal and plant-extract-based synthesis routes, consistent with the visual confirmation criteria.[9,10]

Nanoparticle Characterization Profile

UV-VIS Spectrophotometry Analysis of the Biosynthesized Nanoparticles

The UV–Visible absorption spectra confirmed the successful biosynthesis of copper and magnesium nanoparticles produced using *A. oryzae* cell culture and *Z. officinale* extract (Fig.-2 to 5). The *A. oryzae*-

mediated copper nanoparticles exhibited a characteristic absorption maximum at 550 nm with an absorbance of 1.378, whereas the corresponding magnesium nanoparticles showed a maximum absorption peak at 400 nm with an absorbance of 1.478 (Fig.-2 and 3).

Table-3: Colour Change Observed during the Biosynthesis of Copper and Magnesium Nanoparticles using Fungal Cell Culture and Ginger Extract

Nanoparticle	Source	Colour change observed
Copper (Cu-NPs)	*A. oryzae* cell culture	Blue → Green
Magnesium (Mg-NPs)	*A. oryzae* cell culture	Colourless → Golden
Copper (Cu-NPs)	*Z. officinale* extract	Blue → Green
Magnesium (Mg-NPs)	*Z. officinale* extract	Colourless → Golden

Similarly, the *Z. officinale*-mediated copper nanoparticles displayed a distinct absorption peak at 500 nm with the highest absorbance (1.589) among all synthesized nanoparticles, while the ginger-mediated magnesium nanoparticles exhibited a maximum absorption at 400 nm with an absorbance of 1.278 (Fig.-4 and 5). Overall, the fungal- and plant-mediated copper nanoparticles exhibited different absorption maxima (550 and 500 nm, respectively), whereas both magnesium nanoparticles showed absorption maxima at 400 nm but differed in absorbance intensity. These variations indicate that the biological source influenced the optical properties of the synthesized nanoparticles and suggest differences in nanoparticle formation and physicochemical characteristics.

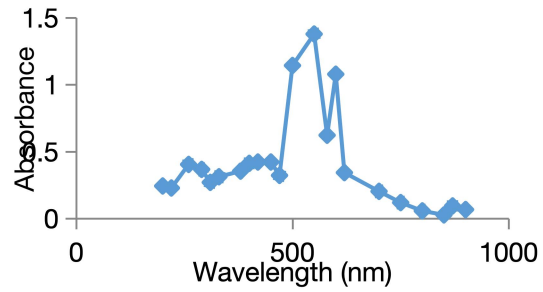


Fig.-2: UV–Vis Spectrum Showing the Absorbance Profile of Copper Nanoparticles Synthesized using *A. oryzae*

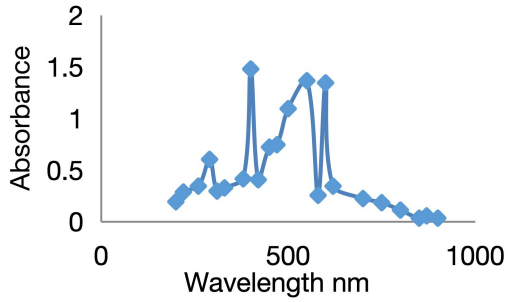


Fig.-3: UV-Vis Spectrum Showing Absorbance of *A. oryzae* Magnesium Nanoparticles

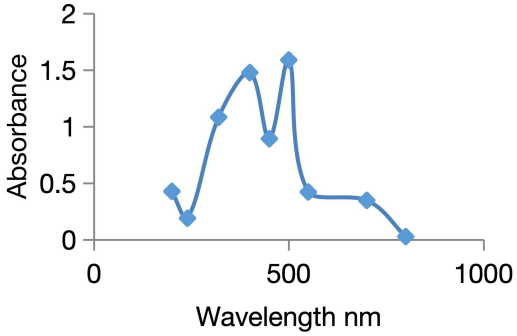


Fig.-4: UV-Vis Spectrum Showing Absorbance of *Z. officinale* Copper Nanoparticles

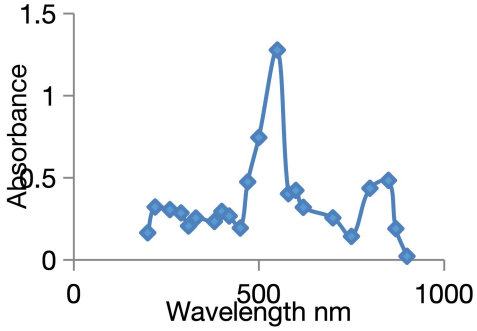


Fig.-5: UV- Vis Spectrum Showing Absorbance of *Z. officinale* Magnesium Nanoparticles (G2)

Fourier Transform Infrared Analysis

Figures 6–9 present the FTIR spectra obtained for the biosynthesised copper and magnesium nanoparticles produced using *Z. officinale* extract and *A. oryzae* cell culture filtrate. A range of absorption bands was detected across the recorded spectra (500-4000 cm^{-1}), reflecting the involvement of both organic and inorganic functional groups in the formation and stabilization of the nanoparticles. In the case of the copper nanoparticles synthesized via *A. oryzae* (Fig.-6), the spectrum revealed distinct bands corresponding to epoxy/oxirane rings, aromatic C–H bonds, tertiary amines, carbonyl-bearing compounds,

aldehydes, aliphatic hydrocarbons, methoxy groups, vinyl C–H bonds, and broad hydroxyl (–OH) stretching. For the magnesium nanoparticles generated using the same fungal filtrate (Fig.-7), bands corresponding to aromatic rings, carbonyl groups, nitriles, methoxy groups, aldehydes, primary amines, and hydroxyl groups were identified. By comparison, the copper nanoparticles synthesized with *Z. officinale* extract (Fig.-8) exhibited a spectrum featuring bands linked to epoxy groups, phenolic hydroxyls, carbonyl compounds, aldehydes, isocyanates, and broad –OH stretching, together with signals characteristic of aromatic ring systems. The ginger-mediated magnesium nanoparticles (Fig.-9), on the other hand, displayed a different band pattern, attributable to ethers, peroxides, alkenes, alkynes, thiols, aldehydes, ammonium ions, and hydroxyl-bearing groups. Overall, hydroxyl (–OH), carbonyl (C=O), aliphatic C–H and nitrogen-containing functional groups were consistently detected across all biosynthesized nanoparticles, although differences in peak positions and functional group composition were observed between the fungal- and plant-mediated nanoparticles. These results imply that biomolecules found in *Z. officinale* extract and *A. oryzae* cell culture played a dual role in the synthesis process, reducing the metal ions while also capping and stabilising the resulting nanoparticles.

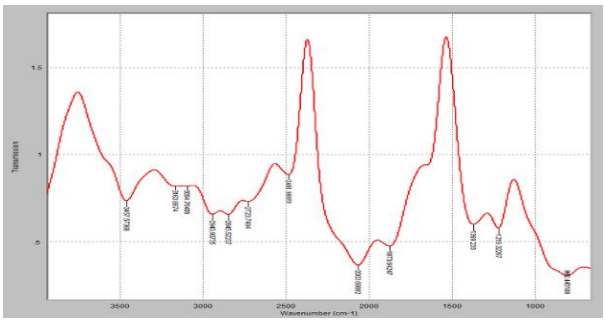


Fig.-6: FTIR Spectrum of the *A. oryzae* Synthesized Copper Nanoparticles.

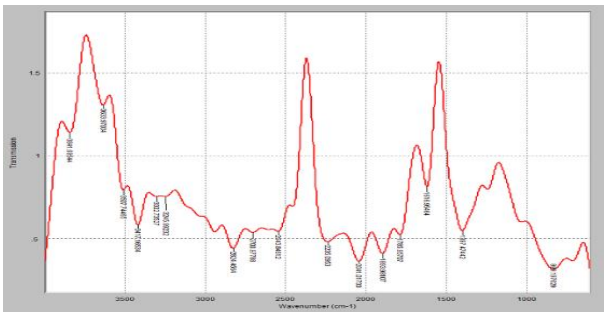


Fig.-7: FTIR Spectrum of the *A. Oryzae* Synthesized Magnesium Nanoparticles

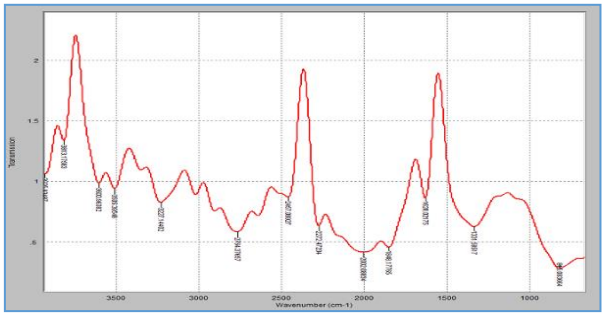


Fig.-8: FTIR Spectrum of the *Zingiber Officinale* Synthesized Copper Nanoparticles

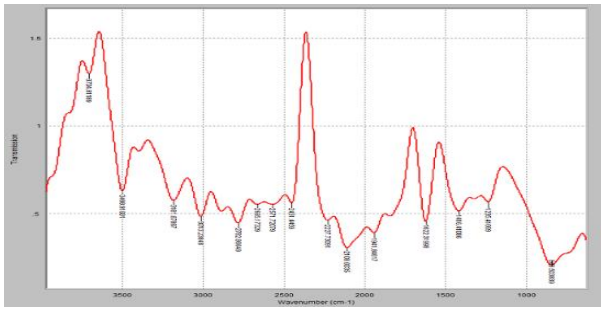


Fig.-9: FTIR Spectrum of the *Zingiber Officinale* Synthesized Magnesium Nanoparticles

X-ray Diffraction Analysis

The X-ray diffraction patterns of the biosynthesized copper and magnesium nanoparticles are presented in Fig.-10 to 13. The diffraction profiles confirmed the crystalline nature of all synthesized nanoparticles, although differences in the number and positions of the diffraction peaks were observed between the fungal- and plant-mediated synthesis routes.

The *Aspergillus oryzae*-mediated copper and magnesium nanoparticles exhibited prominent diffraction peaks at 22.5° and 22.3° (2θ), respectively, corresponding to average crystallite sizes of 7.24 nm and 7.43 nm (Fig.-10 and 11). In contrast, the *Z. officinale*-mediated copper nanoparticles displayed three distinct diffraction peaks at 20.45°, 26.62° and 29.37° (2θ) with a considerably larger average crystallite size of 59.4 nm (Fig.-12). Similarly, the ginger-mediated magnesium nanoparticles exhibited four diffraction peaks at 18.90°, 21.60°, 22.00° and 27.06° (2θ), with an average crystallite size of 23.0 nm (Fig.-13). Overall, the fungal-mediated nanoparticles possessed substantially smaller crystallite sizes than the corresponding ginger-mediated nanoparticles. Among all samples, *A. oryzae*-derived copper nanoparticles

exhibited the smallest crystallite size (7.24 nm), whereas the ginger-derived copper nanoparticles showed the largest crystallite size (59.4 nm). These differences indicate that the biological reducing agents influenced crystal nucleation and growth during nanoparticle biosynthesis.

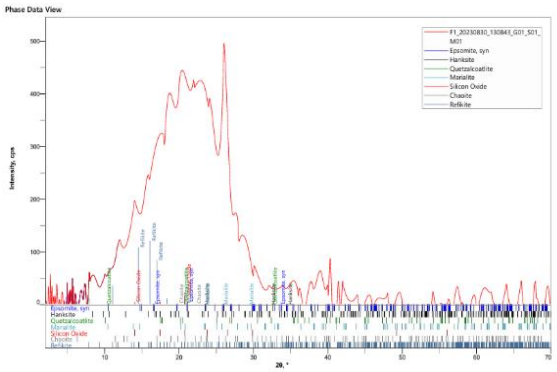


Fig.-10: XRD Graph Showing Diffraction Pattern of *A. oryzae* Synthesized Copper Nanoparticles

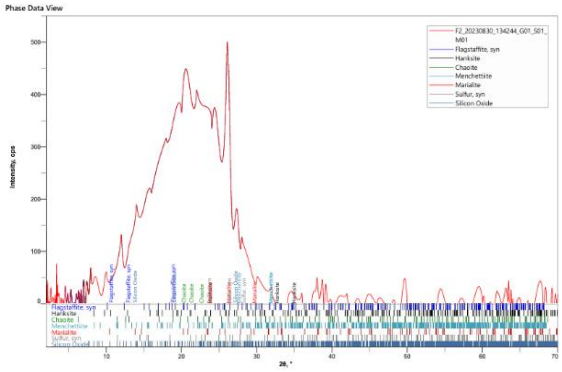


Fig.-11: XRD Graph Showing Diffraction *A. oryzae* synthesized Magnesium Nanoparticles

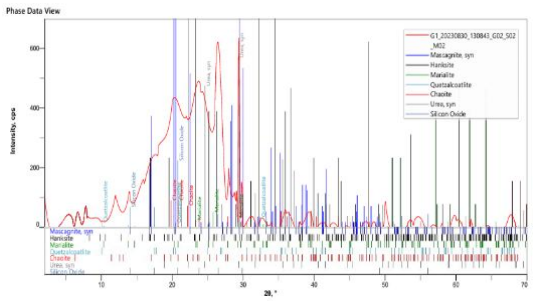


Fig.-12: XRD Graph Showing Diffraction of *Z. officinale* Copper Nanoparticles

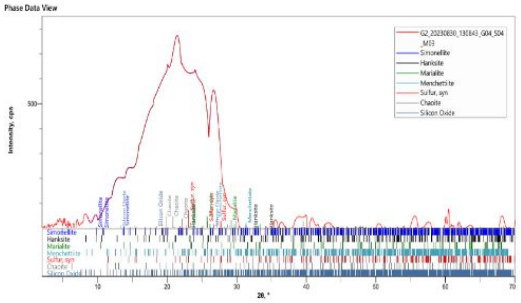


Fig.-13: XRD Graph Showing Diffraction Pattern of *Z. officinale* Synthesized Magnesium Nanoparticles

Scanning Electron Microscope Analysis

The surface appearance and particle size of the biosynthesized copper and magnesium nanoparticles were investigated using SEM. Plates 2–5 display representative SEM micrographs. The micrographs revealed that all synthesized nanoparticles exhibited predominantly irregular morphologies with varying degrees of particle aggregation, although differences in particle size were observed between the fungal- and plant-mediated nanoparticles. The *A. oryzae*-mediated copper nanoparticles (Plate 2) exhibited an average particle diameter of 83.5 nm, whereas the corresponding magnesium nanoparticles (Plate 3) showed a smaller average particle diameter of 50 nm. In comparison, the *Z. officinale*-mediated copper nanoparticles (Plate 4) and magnesium nanoparticles (Plate 5) exhibited average particle diameters of 75 nm and 80 nm, respectively. Overall, the *A. oryzae*-mediated magnesium nanoparticles exhibited the smallest particle size among the four nanoparticle systems, while the *A. oryzae*-mediated copper nanoparticles exhibited the largest average particle diameter. Although all nanoparticles displayed irregular morphologies, the observed differences in particle size and aggregation suggest that the choice of biological reducing agent influenced nanoparticle growth and morphological characteristics during biosynthesis.

Discussion of Molecular Identification, Visual Observation and UV–Vis Spectroscopy

The identification of the isolate as *A. oryzae*, based on a 99.28% sequence similarity, lent support to its potential as a biological reducing agent in nanoparticle synthesis. This organism is recognized for its capacity to secrete large quantities of extracellular enzymes, proteins, polysaccharides, and other secondary metabolites-molecules capable of reducing metal ions while simultaneously stabilizing the nanoparticles formed. These extracellular biomolecules function as natural capping agents, promoting nanoparticle assembly and enhancing their stability. Such properties position *A. oryzae* as a promising, cost-effective, and eco-friendly alternative to conventional chemical synthesis methods.

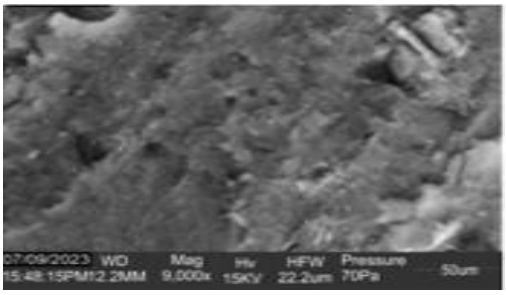


Plate-2: SEM images of *A. oryzae* Synthesized Copper Nanoparticles

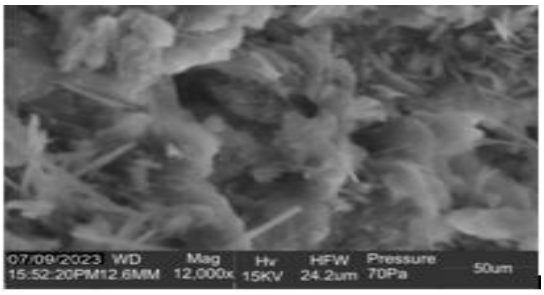


Plate-3: SEM images of *A. oryzae* Synthesized Magnesium Nanoparticles

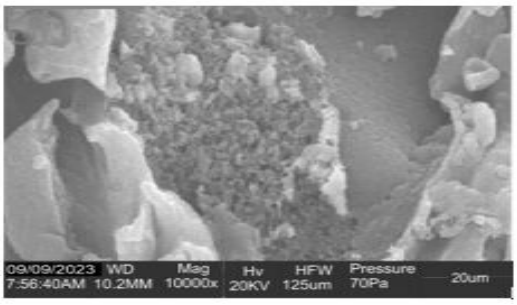


Plate-4: SEM images of *Z. officinale* Synthesized Copper Nanoparticles

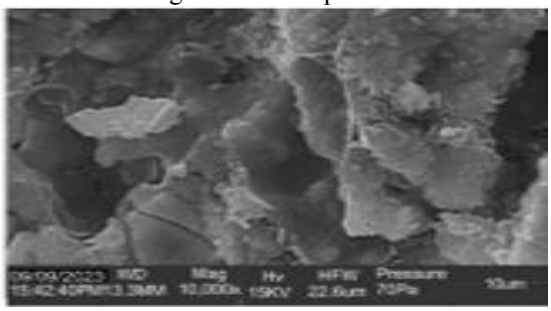


Plate-5: SEM images of *Z. officinale* Synthesized Magnesium Nanoparticles

This aligns with findings from other studies, which have similarly identified fungi as efficient biological nanofactories,[7,11-13] attributing their strong biosynthetic capability to a metabolite-rich extracellular profile and the relative ease with which they can be cultured at scale. The observed colour transitions-from blue to green for the copper nanoparticles and from colourless to golden for the magnesium nanoparticles-served as an early qualitative marker of successful synthesis. These shifts are characteristic of the reduction of metal ions into their nanoparticle form, arising from optical changes associated with surface plasmon resonance, a phenomenon similarly reported in other studies involving the green synthesis of metallic nanoparticles using *Z. officinale* and comparable biological agents.[14-17] The fact that both the fungal culture filtrate and the ginger extract successfully facilitated nanoparticle formation lends further support to the reliability of biological metabolites as reducing and stabilizing agents, reinforcing the growing preference for green synthesis approaches over traditional chemical methods.[18,19] The UV–Visible spectra further confirmed nanoparticle formation through the appearance of characteristic absorption peaks. The *A. oryzae*-derived copper nanoparticles exhibited maximum absorption at 550 nm, whereas ginger-derived copper nanoparticles showed a peak at 500 nm. In contrast, magnesium nanoparticles synthesized from both biological sources displayed absorption maxima at approximately 400 nm, although differences in absorbance intensity were observed. These variations indicate that the biological source influenced nanoparticle nucleation, particle size, morphology, and surface chemistry during synthesis. Previous studies have similarly reported that phytochemicals present in ginger extracts and extracellular fungal metabolites significantly affect the optical characteristics and stability of biosynthesized nanoparticles.[14-16,20] The stronger absorbance recorded for the ginger-mediated copper nanoparticles could point to a higher nanoparticle concentration or better dispersion, plausibly driven by the abundance of phenolics, flavonoids, and gingerols acting as efficient reducing agents. Taken together, these differences underline how much the choice of biological reducing agent shapes the physicochemical characteristics and downstream applications of biosynthesized nanoparticles.[1,12,13] Overall, the molecular identification, visual observations, and UV–Vis analyses collectively confirmed the successful biosynthesis of copper and magnesium nanoparticles using both *A. oryzae* cell culture and *Zingiber officinale* extract. The findings demonstrate that both biological systems provide effective green synthesis platforms capable of producing stable nanoparticles with distinct optical properties suitable for potential biomedical, agricultural, and environmental applications, including wastewater treatment and sustainable crop production.[21-23]

Discussion of FTIR and XRD Analyses

Collectively, the FTIR results demonstrated that both the *Aspergillus oryzae* cell culture filtrate and the *Zingiber officinale* extract contained a diverse array of biomolecules actively involved in shaping and stabilising the copper and magnesium nanoparticles. Detection of hydroxyl (–OH), carbonyl (C=O), amine (–NH), methoxy, aldehyde, and aromatic functional groups indicated that proteins, phenolic compounds, polysaccharides, and other secondary metabolites contributed to the reduction and stabilisation processes throughout nanoparticle synthesis. In addition to facilitating the reduction of metal ions, these biomolecules appeared to restrict excessive particle aggregation, thereby contributing to greater nanoparticle stability. This pattern is consistent with previous reports on fungal- and plant-based nanoparticle synthesis, where hydroxyl, carbonyl, and amine groups have similarly been highlighted as the principal functional groups driving nanoparticle formation and stabilisation.[4, 13-15] The minor variations in functional-group composition observed between the fungal- and ginger-derived nanoparticles are likely attributable to differences in the underlying biochemical composition of the two reducing agents, which may in turn account for the variation observed in their physicochemical characteristics. XRD data confirmed the crystalline nature of every synthesized sample, demonstrating that metal ions had been successfully converted into crystalline nanostructures. Crystallite sizes were noticeably smaller for the fungal-mediated copper and magnesium nanoparticles (7.24 and 7.43 nm) than for their ginger-mediated counterparts (59.4 and 23.0 nm), pointing to *A. oryzae* metabolites being more effective at driving crystal nucleation while holding crystal growth in check. Smaller, more well-formed crystallites of this kind are advantageous, since reduced crystallite dimensions tend to boost surface area, catalytic activity, and biological performance. This pattern echoes other work on biologically synthesized metallic nanoparticles, where the choice between fungal metabolites and plant phytochemicals has been shown to strongly shape crystal formation, crystallite size, and durability.[7,17-20] In short, both biological routes yielded stable crystalline nanoparticles according to the FTIR and XRD data, though *A. oryzae* came out ahead in producing nanoparticles with finer crystallite structures, a trait that could translate into greater potential for biomedical, environmental, and wastewater-treatment use.[21,23]

Discussion of SEM Analysis, Comparative Evaluation, and Study Implications

Irregular morphology with varying degrees of aggregation was evident across all the SEM micrographs, a pattern typical of biologically synthesized metallic nanoparticles. This aggregation is best explained by the high surface energy of the nanoparticles combined with interactions among the biomolecules adsorbed on their surfaces during synthesis. Even so, the particle sizes recorded (50–83.5 nm) sit comfortably within the nanoscale range and align with values reported elsewhere for fungal- and ginger-mediated metallic nanoparticles.[13,14,20] The smaller particle size seen with the *A. oryzae*-mediated magnesium nanoparticles points to fungal metabolites exerting tighter control over particle growth than the ginger extract does, consistent with reports that extracellular fungal proteins and enzymes help regulate nanoparticle stabilization and size.[11,12] Weighing the two systems against each other, both *A. oryzae* cell culture and *Z. officinale* extract synthesized copper and magnesium nanoparticles successfully, though the two routes diverged in optical properties, crystallite size, functional groups, and particle morphology. Fungal-mediated synthesis yielded smaller crystallites and particles, while the ginger-mediated nanoparticles registered higher UV–Vis absorbance a divergence that traces back to differences in the reducing and capping capacity of fungal metabolites versus plant phytochemicals. Comparable variation has turned up in other comparative studies of green nanoparticle synthesis, where the makeup of the biological reducing agent strongly shaped nanoparticle characteristics and stability.[15,17,19] Both biological routes emerge from this work as environmentally friendly alternatives to conventional chemical synthesis, with real promise for biomedical, agricultural, and environmental use. Nanoparticles that are smaller and stable are especially well suited to catalytic work, antimicrobial formulations, and wastewater treatment, given their larger surface area and heightened reactivity.[21,23] Using consistent analytical protocols throughout adds confidence to the physicochemical characterization reported here.[25] One limitation is that the comparison of fungal- and plant-mediated routes here stopped at physicochemical characterization; a natural next step would be testing the antimicrobial, antioxidant, cytotoxic, catalytic, and wastewater-remediation performance of these nanoparticles to gauge their real-world applicability under laboratory and field

conditions.[23] Taken as a whole, this study confirms *A. oryzae* cell culture and *Z. officinale* extract both function as effective green reducing agents for copper and magnesium nanoparticle biosynthesis. That said, the fungal route came out ahead in producing smaller, more crystalline nanoparticles, suggesting it may be the more efficient platform for sustainably manufacturing nanomaterials across industrial, biomedical, and environmental settings.

CONCLUSION

This study successfully demonstrated the comparative green synthesis of copper and magnesium nanoparticles using *A. oryzae* cell culture filtrate and *Z. officinale* extract as biological reducing agents. Both biosynthetic routes yielded stable nanoparticles, as confirmed through SEM, FTIR, XRD, and UV–Vis analyses. Notably, synthesis mediated by *A. oryzae* produced nanoparticles with smaller crystallite and particle sizes, indicating greater control over the nanoparticle formation process. These outcomes highlight the potential of fungal- and plant-based synthesis as simple, cost-effective, and environmentally friendly alternatives to conventional chemical synthesis techniques. Future research should prioritise investigating the biological activities and practical applications of the synthesised nanoparticles, particularly within agriculture, medicine, and environmental remediation.

ACKNOWLEDGMENTS

The authors are grateful to PerfectGlory Scientific and Environmental Laboratory Services Limited NNEWI for providing the Laboratory facility for this work

CONFLICT OF INTERESTS

The authors declare that no conflict of interest exists.

AUTHOR CONTRIBUTIONS

The present work is related to *SDG-9: Industry, Innovation and Infrastructure*. All the authors contributed significantly to this manuscript, participated in reviewing/editing and approved the final draft for publication. The research profile of the authors can be verified from their ORCID ids, given below:

Nwamaka Anthonia Dibua https://orcid.org/0009-0007-6988-2047
Edna Ifeoma Chukwura https://orcid.org/0009-0000-4127-9253
Ifeyinwa Oslar Emmy- Egbe https://orcid.org/0009-0008-4175-3515
Obidimma Bright Uba https://orcid.org/0000-0001-5538-2403
Okwukweka Favour Nwajiobi https://orcid.org/0009-0002-0412-2163
Ifeoma Susan Ezenwata https://orcid.org/0009-0009-37652989
Obianuju Helen Obiefuna https://orcid.org/0000-0002-5527-3968
Elochukwu Chidubem Sunday Okoye https://orcid.org/0000-0002-1568-1887
Jude Chukwudi Chikwendu https://orcid.org/0009-0000-6081-0118
Chinyere Lilian Eleanya https://orcid.org/0000-0002-4699-8887
Stella C. Afulukwe https://orcid.org/0009-0009-9152-4726
Chukwuebuka Egbuna http://orcid.org/0000-0001-8382-0693

Open Access: This article is distributed under the terms of the Creative Commons Attribution 4.0 International License (http://creativecommons.org/licenses/by/4.0/), which permits unrestricted use, distribution, and reproduction in any medium, provided you give appropriate credit to the original author(s) and the source, provide a link to the Creative Commons license, and indicate if changes were made.
Cite this article as: N. A. Dibua *et al.*, *Rasayan J. Chem.*, Vol.19, Special Issue, 197-207(2026), https://doi.org/10.31788/RJC.2026.19510105

REFERENCES

1. K. A. Altammar, Frontiers in Microbiology, **14,** 1155622(2023), http://doi.org?10.3389/fmicb.2023.1155622
2. S. Anjum, M. Hashim, S. A. Malik, M. Khan, J. M. Lorenzo, B. H. Abbasi, and C. Hano, *Cancers*, **13**, 4570(2021), https://doi.org/10.3390/cancers13184570

3. V. Dhapte, and V. Pokharkar, 2019, Nanosystems for drug delivery: Design, engineering, and applications. In A. K. Shukla and S. Iravani (Eds.), *Green Synthesis, Characterization and Applications of Nanoparticles*, Elsevier, pp. 321–345, https://doi.org/10.1016/B978-0-08-102579-6.00013-5
4. S. Mehrotra, V. Goyal, C. O. Dimkpa, and V. Chhokar, *Plants*, **13(9)**, 1255(2024), https://doi.org/10.3390/plants13091255
5. G. Karunakaran, K. G. Sudha, S. Ali, and E. B. Cho, *Molecules*, **28(11)**, 4527(2023), https://doi.org/10.3390/molecules28114527
6. C. Egbuna, V. K. Parmar, J. Jeevanandam, S. M. Ezzat, K. C. Patrick-Iwuanyanwu, C. O. Adetunji, J. Khan, E. N. Onyeike, C. Z. Uche, M. Akram, M. S. Ibrahim, N. M. El Mahdy, C. G. Awuchi, K. Saravanan, H. Tijjani, U. E. Odoh, M. Messaoudi, J. C. Ifemeje, M. C. Olisah, N. J. Ezeofor, C. J. Chikwendu, and C. G. Ibeabuchi, *Journal of Toxicology*, **Article 9954443**, 1–21(**2021),** https://doi.org/10.1155/2021/9954443
7. B. Koul, A. K. Poonia, D. Yadav, and J. O. Jin, *Biomolecules*, **11(6)**, 886(2021), https://doi.org/10.3390/biom11060886
8. A. Boroumand Moghaddam, F. Namvar, M. Moniri, P. Md Tahir, S. Azizi, and R. Mohamad, *Molecules*, **20(9)**, 16540(2015), https://doi.org/10.3390/molecules200916540
9. K. O. Shittu and O. Ihebuna, *Advanced Natural Sciences,* **8**, 045003(2017), http://doi.org/10.1088/2043-6254/aa8536
10. M. T. Moustafa, *Water Science,* **31,** 164(2017), https://doi.org/10.1016/j.wsj.2017.11.001
11. U. R. Ezeilo, R. A. Wahab, L. C. Tin, I. I. Zakaria, F. Huyop, and N. A. Mahat, *Waste and Biomass Valorization*, **11**(**7**), 3133(2020), https://doi.org/10.1007/s12649-019-00665-4
12. S. P. K. Malhotra, and M. A. Alghuthaymi, 2022, Biomolecule-assisted biogenic synthesis of metallic nanoparticles. In *Agro-Waste and Microbes for Production of Sustainable Nanomaterials*, Springer, Cham, **21,** pp. 139–163, https://doi.org/10.1007/978-3-319-98708-8_1
13. S. C. Kumari, V. Dhand, and P. N. Padma, *Nanomaterials*, **11**, 259(2021), https://doi.org/10.3390/nano11020259
14. O. Hari, S. Nabin, K. C. Ekaraj, S. Anup, and T. Rajan, *Journal of Nepal Chemical Society*, **39**, 10(2018), https://doi.org/10.3126/jncs.v39i0.24561
15. S. Jadoun, R. Arif, N. K. Jangid, and R. K. Meena, *Environmental Chemistry Letters*, **19**, 355(2021), https://doi.org/10.1007/s10311-020-01148-4
16. A. Kamal, S. Zaki, H. Hassan, and D. Abdelhaleem, *Journal of Pure and Applied Microbiology*, **14**, 1227(2020), https://doi.org/10.22207/JPAM.14.2.35
17. G. Pal, P. Rai, and A. Pandey, 2019, Green synthesis of nanoparticles: A greener approach for a cleaner future. In A. K. Shukla and S. Iravani (Eds.), *Green Synthesis, Characterization and Applications of Nanoparticles*, Elsevier, pp. 1–26. https://doi.org/10.1016/B978-0-08-102579-6.00001-3
18. S. Sim, N. K. Wong. *Biomedical Reports*, **14**, 42(2021), https://doi.org/10.3892/br.2021.1418
19. I. Khan, K. Saeed, and I. Khan, *Arabian Journal of Chemistry*, **12**, 908(2019), https://doi.org/10.1016/j.arabjc.2017.05.011
20. R. D. More, and D. M. Janrao, *International Journal for Research in Applied Science and Engineering Technology*, **9**(**7**), 429(2021), https://doi.org/10.22214/ijraset.2021.36034
21. I. Haidri, M. Shahid, S. Hussain, T. Shahzad, F. Mahmood, U. M. Hassan, M. J. Al-Khayri, M. I. Aldaej, M. N. Sattar, A. A. Rezk, A. M. Almaghasla, and W. F. Shehata, *Plants*, **12**, 3058(2023), https://doi.org/10.3390/plants12173058
22. A. Owhonka, O. G. Okundaye, W. Ekongson, A. H. Isaac, and I. Harold, *Juvenis Scientia*, **10**(**3**), 26(2024), https://doi.org/10.32415/jscientia_2024_10_03_26-37
23. S. Waqas, N. Y. Harun, N. S. Sambudi, M. R. Bilad, K. J. Abioye, A. Ali, and A. Abdulrahman, *Water*, **15**, 1913(2023), https://doi.org/10.3390/w15101913

[RJC-10105/2026]